Journal of Materials Chemistry C

Accepted Manuscript

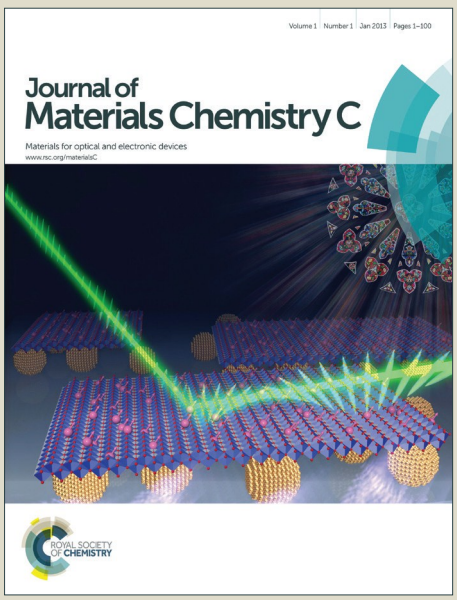

ROYAL SOCIETY OF CHEMISTRY

www.rsc.org/materialsC

Journal Name

ARTICLE

Spiropyrane-induced One-dimensional Cyclodextrin Microcrystals with Light-driven Fluorescence Change

Received 00th January 20xx,

Accepted 00th January 20xx

DOI: 10.1039/x0xx00000x

www.rsc.org/

Baozhong Lv,[a] Zhen Wu,[a] Chendong Ji,[a] Wantai Yang,[a] Dongpeng Yan*[b] and Meizhen Yin*[a]

Systems on light-driven fluorescence change have received much attention due to their applications in luminescent switches or as sensors. However, such solid-state systems are still limited relative to those in the solution form, and how to obtain photochromic fluorescent film materials toward device fabrication is a long-time problem. In this work, one-dimentioanal (1D) solid-state microcrystals combining the host cyclodextrin (**CD**) and UV-responsive guest molecule spiropyran (**SP**) have been developed, which present a light-driven fluorescence change based on the isomerization of the **SP** molecule in the **CD** matrix**.** Firstly, the supramolecule forces including inherent hydrogen bondings and hydrophobic interaction in this self-assembled system was studied by electrospray ionization mass spectrometry (ESI-MS), isothermal titration calorimetry (ITC), and Fourier transform infrared spectra (FTIR). The scanning electron microscopy (SEM) comparison between the **SP@CD** system and the pristine **CD** or **SP** confirms that the **SP** guest plays a crucial role in the formation of 1D microcrystals. Then, through a spin-casting process, the thin film of **SP@CD** microcrystals was further fabricated, which shows a reversible photochromic fluorescence between fluorescence-free and high red-emission states. Moreover, the open-ring form of **SP@CD** microcrystals also presents two-photon emission and polarized fluorescence. Therefore, this work has offered a facile way to obtain reversible photochromic fluorescent film, which may be applied in dynamic light-controlled fluorescent sensor and two-photon imaging.

1. Introduction

Recently, molecule-based solid-state luminescent materials have received great attention due to their promising photofunctional applications in the fields of light-emitting diodes,[1] lasers,[2] sensors,[3] and two-photon fluorescent materials.[4] In terms of fundamental studies and practical applications, the ability to tune and control the luminescence (such as color and intensity) of the molecular solid materials is important to achieve multi-color fluorescence[5] and dynamic light-emitting switches.[6] In this context, light-driven fluorescent change (also known as photochromic fluorescence (**PCF**)) has supplied an effective way to achieve tunable luminescence upon light irradiation, and **PCF** materials have also been paid attention recently due to their potential applications in fluorescent switches, information storage, and optical communication fields.[7] However, compared with the photochromic materials that solely switches the absorption spectra (i.e. color) between two alternative states, the study of **PCF** materials is still in an early stage and needs to be developed.

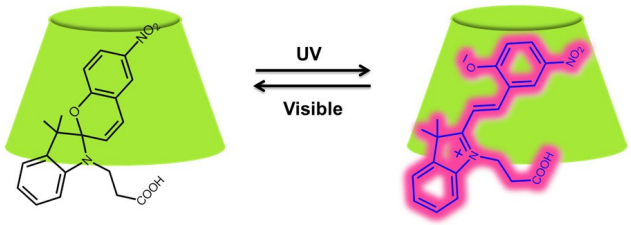

Scheme 1 Chemical structures of **SP-COOH** and photoisomerization of **SP-COOH** incorporated in **γCD**.

Spiropyran (**SP**) molecule is a promising photochromic compound that possesses controllable color change due to the reversible structural transformations in response to light.[8-11] However, since the interconversion between closed-form **SP** and the open-form photomerocyanine (**PM**) involves a large molecular rearrangement, it is rather difficult to achieve the photochromism and **PCF** properties for the pristine **SP** in the solid-state form.[12] To achieve a dynamic transformation between **SP** and **PM**, **SP**s are commonly included into polymer matrices, zeolites and the clays to obtain solid-state photochromic materials (such as fibers, films, beads, and

[a] State Key Laboratory of Chemical Resource Engineering, Beijing Laboratory of Biomedical Materials, Beijing University of Chemical Technology, Beijing 100029, China. Email: yinmz@mail.buct.edu.cn
[b] Key Laboratory of Theoretical and Computational Photochemistry, Ministry of Education, College of Chemistry, Beijing Normal University, Beijing 100875, P. R. China. Email: yandp@bnu.edu.cn
† Electronic Supplementary Information (ESI) available: See
DOI: 10.1039/x0xx00000x

crystals).[13, 14] As an important type of host matrix during the development of host-guest chemistry, cyclodextrins (**CD**s) have also won the favor of scientists due to their hydrophilic exterior and hydrophobic interior, which not only possess inclusion and recognition abilities on functional guest molecules, but also offer a unique opportunity to study size controlled nano-environment effect on spectroscopy, kinetics, etc.[15] For example, Arima *et al.*[16] found that **SP**s can be included in γ-cyclodextrin (**γCD**) and exhibit photochromism in a solid-state form, because the **γCD** cavity has sufficient free volume to allow interconversion of **SP**. However, to the best of our knowledge, the detail study on variations of **CD** micro-morphology induced by **SP** and the solid-state crystalline characteristics have not been reported. Moreover, the incorporation of **SP** into **γCD** matrix can also serve as a model system to understand molecular self-assembly of host-guest system at the micro/nanometer scale.

In this work, we report the reversible **PCF** materials based on one-dimensional micro-sized crystals constructed by arrayed assembly of **SP-COOH@γCD**. 3-(3',3'-dimethyl-6-nitrospiro[chromene-2,2'-indolin]-1'-yl)propanoic acid (**SP-COOH**) (Scheme 1) was chosen as the guest molecule based on the fact that the free carboxyl can form potential hydrogen-bond with the hydroxy from **γCD**, and the molecular size of **SP-COOH** is matching well the inclusion into **γCD**. Moreover, the high fluorescence quantum yield for **SP-COOH** (Φ_F=9.79% in solution; λ_{ex}=540 nm and λ_{em}=635 nm) is also benefit to obtain high fluorescent on/off contrast during the photoisomerization process. It was observed that the **SP-COOH** facilitated the formation of one-dimensional microcrystals with **γCD**, which is lack for the single isolate **γCD** or **SP-COOH**, suggesting that the hydrogen bonding interaction between –COOH group in **SP-COOH** and –OH group in **γCD** may play a key role during the self-assembly process. Through a spin-casting method, **SP@γCD** thin film has also been constructed, which presents a UV-induced fluorescent response with the fluorescence change at different irradiation time. Additionally, the two-photon emission and polarized fluorescence can also be obtained for the open-ring state of **SP-COOH@CD**. Therefore, this work not only presents a detailed study on the micro-sized host-guest solid-state crystalline materials, but also supplies a deep understanding on the **PCF** behaviors toward practical light-switching application.

2. Experimental Section

2.1 Reagents and materials

3-Methyl-2-butanone (98%), 3-iodopropanoic acid (98%), bromoethane (98%), 2-iodoethanol (98%), phenylhydrazine hydrochloride (98%) and 2-hydroxy-5-nitrobenzaldehyde (98%) were purchased from Alfa Aesar Chemical. Co. Ltd. and used without further purifications. **βCD** and **γCD** (98%) was purchased from Aladdin Chemical. Co. Ltd. All solvents were dried prior to use with appropriate drying agents. Analytical thin layer chromatography (TLC) was carried out on Yantai chemical industry silica gel plates.

2.2 Synthesis and complex of SP-COOH with γCD

The detailed synthesis process of **SP-COOH** is described in Supporting Information (Scheme S1). The structure of **SP-COOH** has been confirmed by NMR (Fig. S1-S3). In order to prepare the complex of **SP-COOH** with **γCD**, **γCD** (650mg, 0.5mmol) was dissolved in water (25 mL), and then a solution of **SP-COOH** (38 mg, 0.1mmoL) in ethanol (2 mL) was added into **γCD** solution under vigorous stirring. A precipitation was observed instantly. After stirring at room temperature for 12 h, the mixture was kept at 4 °C for 24 h. Then, the obtained precipitation was filtered out, washed with 5 mL of cold water-ethanol solvent (40% v/v) for three times, and then dried at room temperature in vacuum in the dark overnight to afford a pale yellow complex (**SP-COOH@γCD)**. The solid film of **SP-COOH@γCD** was prepared by a spin-casting method. The as-obtained powder of **SP-COOH@γCD** was dispersed in water and then was deposited onto a quartz plate and dried at room temperature in vacuum overnight. Finally, a pale yellow film was obtained for subsequent detection, the SEM of **SP-COOH@γCD** film is given in Fig. S4.

2.3 Sample characterization

^{1}H-NMR spectra were recorded on a Bruker 400 (400 MHz ^{1}H; 100 MHz ^{13}C) spectrometer at room temperature. Mass spectra (MS) were measured with a XEVO-G2QTOF (ESI) (Waters, USA). High resolution transmission electron microscopy (HRTEM) images were obtained with a JEOL JEM-2100 high resolution transmission electron microscope (the accelerating voltage was 200 kV). X-ray diffraction (XRD) patterns of the powder were recorded using a Rigaku 2500VB2+PC diffractometer using the Cu Kα radiation (λ=1.541844 Å) at 40 kV and 50 mA with the step-scanned mode in 0.04° (2θ) per step and count time of 10s/step in the range from 5 to 40°. Thermogravimetric analysis (TGA) was conducted on TGA/SDTA851e thermosbalance with a heating rate of 10 °C/min. Nano ITC (TA Instruments Waters, LLC, UT) was used for isothermal titration calo-rimeter (ITC) experiments. Fourier transform infrared (FT-IR) spectra were recorded using a Thermo Nicolet Nexus FT-IR devise with the Smart Golden Gate ATR attachment in the range of 4000−500 cm^{-1} with 2 cm^{-1} resolution. Fluorescence spectroscopic studies were performed on a fluorescence spectrophotometer (Horiba JobinYvon FluoroMax-4 NIR, NJ, USA). UV-visible spectra were obtained on a spectrometer (Cintra 20, GBC, Australia). The percentage contribution of each lifetime component to the total decay curve, polarized fluorescence and photoluminescence quantum yield (PLQY) were recorded using an Edinburgh Instruments' FLS 980 fuorospectrophotometer. The surface morphology was investigated by a Zeiss Supra 55 and HITACHI S-4700 (Japan) scanning electron microscope (the accelerating voltage was 20 kV). Fluorescence microscopy image was recorded on a Broadband Confocal and Multiphoton Microscope (TCS SP5MP) with a two-photon near-infrared pulse laser at 800 nm.

Journal Name

ARTICLE

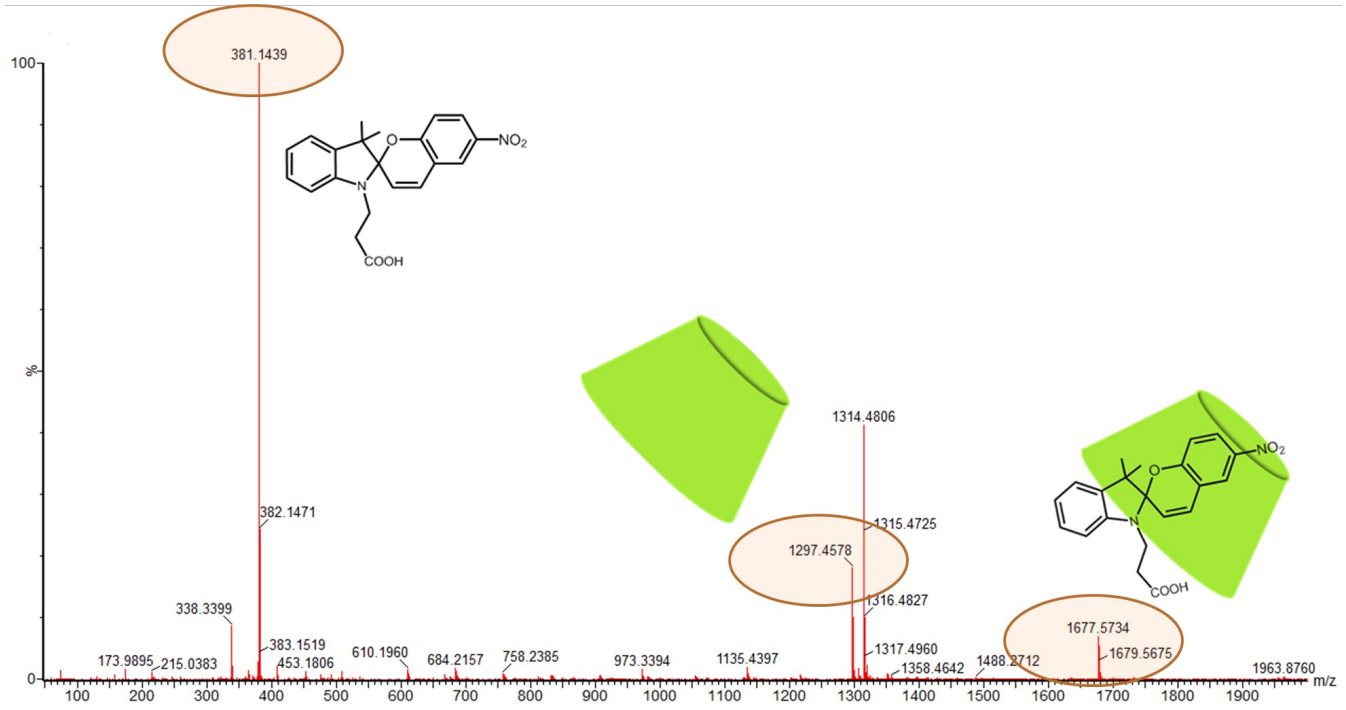

Fig. 1 ESI-MS spectrum of **SP-COOH@γCD**.

3. Results and Discussion

3.1 Host-guest structure and solid-state morphology

The synthesis and characterization of **SP-COOH** can be found in supporting information (Scheme S1 and Fig. S1-S3). Electrospray ionization mass spectrometry (ESI-MS) is an effective technique to detect the non-covalent interaction, which also provides molecular weight information that allows determining the detailed stoichiometry. In the ESI-MS spectrum of the as-prepared sample of **SP-COOH@γCD** (Fig. 1), the peaks observed at m/z=381.1439, 1297.4578 and 1677.5734 correspond to **SP-COOH**, **γCD** and **SP-COOH@γCD** (theoretical m/z=381.1450, 1297.4304, 1677.5676), respectively. The MS data revealed apparently that the ratio of host to guest is 1:1 for the inclusion complex, and this is compatible with the previous work.[17, 18] The ratio of host to guest for the inclusion complex was also verified by ^{1}H-NMR of **SP-COOH@γCD** (Fig. S5). Taking the size of **SP-COOH** (Scheme 2A) and **γCD** (Scheme 2B, torus height of 7.8 Å and inner torus diameter of 9.5Å at the wide rim) [19] into account, the cavity of **γCD** is not large enough to accommodate two **SP-COOH** molecules at the same time, which is consistent well with above-mentioned ESI-MS result. To detect the host-guest recognition between **SP-COOH** with other **CD** system, **βCD** was also chosen as the inclusion matrix for comparison. As shown in Fig. S6, the lack of the peak for **SP-COOH/βCD** complex in the ESI-TOF spectrum indicates that **SP-COOH** and **βCD** hardly formed a stable complex, and **βCD** can be washed out with water. Therefore, **γCD** presents a highly selective recognition for **SP-COOH** molecule than **βCD**. As well, the host-guest structure and thermophysical properties of **SP-COOH@γCD** were studied in supporting information by NMR (Fig. S7), XRD (Fig. S8) and TGA (Fig. S9). The results of pristine **SP-COOH** and **γCD**, the physical mixture of **SP-COOH** and **γCD** (1:1, mol/mol), and the complex inclusion **SP-COOH@γCD** showed that the patterns of the inclusion complex were different from those of the physical mixture, confirming the formation of host–guest structure.

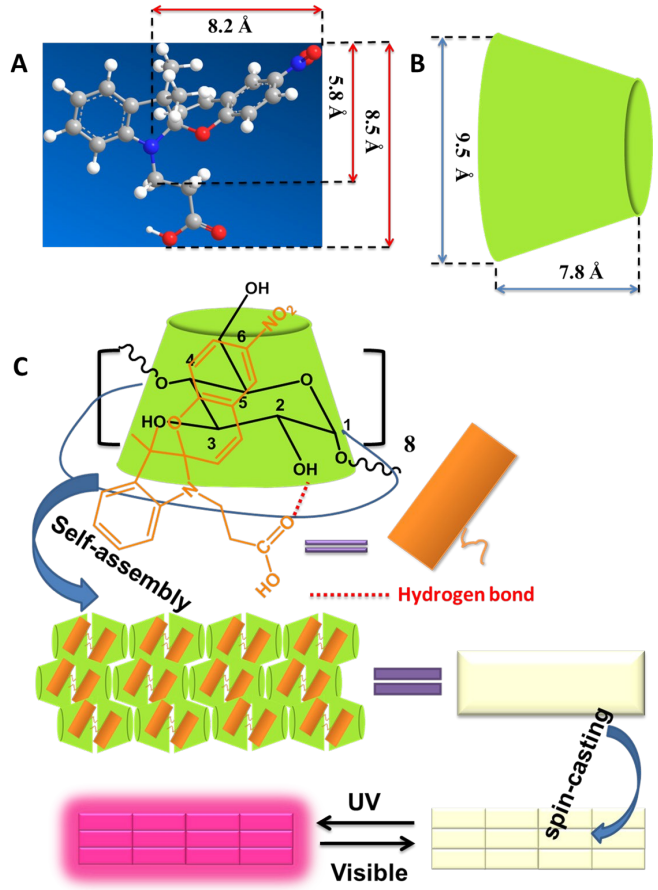

Scheme 2 Geometric conformations and sizes of (A) **SP-COOH** and (B) **γCD**. (C) The illustration of the incorporation of **SP** into **γCD** (**SP-COOH@γCD**) and the fabrication of **SP-COOH@γCD** solid film.

The morphology of the obtained **SP-COOH@γCD** supramolecular assembly was further studied by both scanning electron microscopy (SEM) and transmission electron microscopy (TEM) images (Fig. 2A and 2B). SEM image shows that **SP-COOH@γCD** presents a well-organized 1D rod-like microcrystal structure (Fig. 2A). TEM image further confirms the typical **SP-COOH@γCD** microcrystals with the length of 5-10 μm and width of 1-2 μm (Fig. 2B). XRD studies allow the identification of the structure for **SP-COOH@γCD** complexes. Fig. S8 shows the main peak of **γCD** is retained upon the inclusion of **SP-COOH** guest, which suggests the host framework of **SP-COOH@γCD** is similar to that of the pristine **γCD**. The lack of the peak belonging to **SP-COOH** suggests that there is no phase separation between **SP-COOH** and **γCD**. To further detect the role of **SP-COOH** guest in the formation of 1D micro-sized crystals, SEM images of pristine **SP-COOH** and **γCD** were further studied under the same condition as the preparation of **SP-COOH@γCD**. Both the images of pristine **SP-COOH** and **γCD** showed unordered aggregation morphology (Fig. S10). Thus, **SP-COOH** guest molecule can induce **γCD** host to the formation of 1D microcrystals, and the self-assembly mode for the **SP-COOH@γCD** can be illustrated in Scheme 2C, in which the introduced **SP-COOH** molecule plays an important role to regularize the assembled process, and the assembled pattern of **γCD** is also maintained.

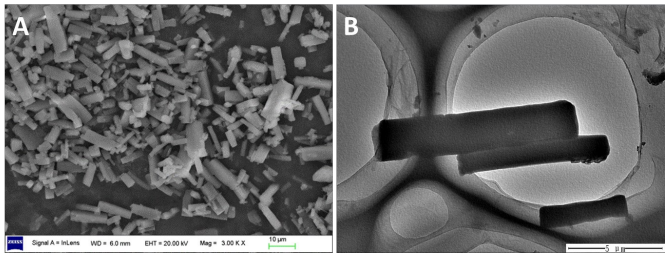

Fig. 2 (A) SEM and (B) TEM images of **SP-COOH@γCD**.

3.2 Interaction between SP-COOH and γCD

To evaluate the major driving force functioned in this host-guest system, the thermodynamic parameters of **SP/γCD** were quantified by isothermal titration calorimetry (ITC). The acquired titration curves and thermodynamic parameters are given in Fig. 3. The negative value of free energy (ΔG) indicates the incorporation process is spontaneous. The negative values of ΔH and ΔS, and the affinity constants (Ka) of 2.003×10^5 M^{-1} are calculated by Nano ITC software, indicating the strong hydrogen bonds accompanied with hydrophobic interaction are the leading factor in this complex system.[20]

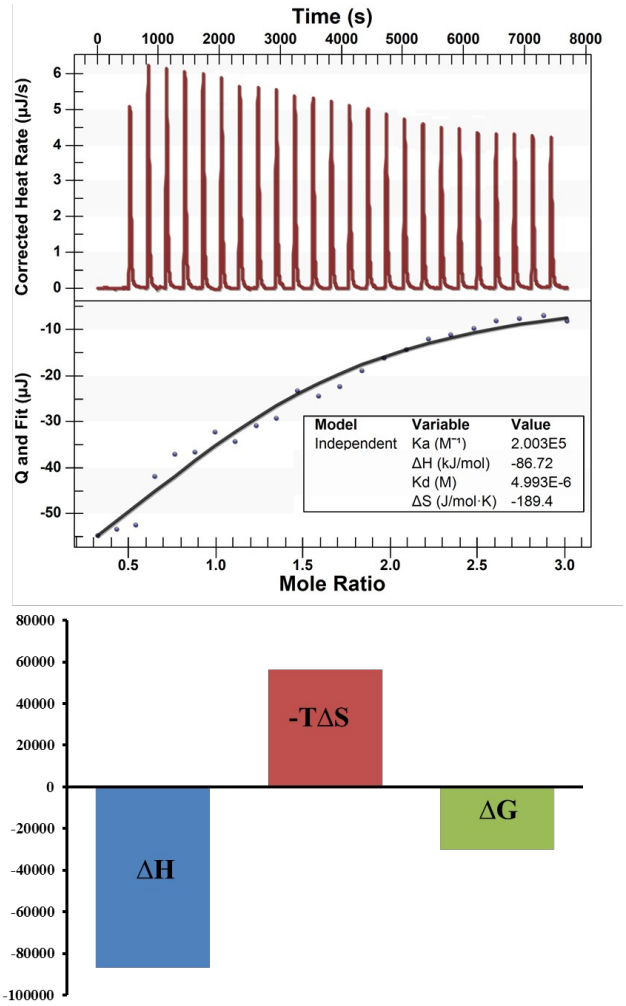

Fig. 3 Heat effects measured by ITC in the titration of **γCD** and **SP-COOH** aqueous solutions.

To further obtain the information on the interaction modes between **CD** and **SP-COOH**, FTIR spectra were measured for both the self-assembled **SP-COOH@γCD** and their precursors (Fig. 4). In the FTIR spectrum of the pristine **γCD**, the characteristic absorption bands at around 1024 cm^{-1} and 1078 cm^{-1}, correspond to the coupled C–C and C–O stretching vibrations; the absorption band at around 1160 cm^{-1} can be attributed to the anti-symmetric stretching vibration of the C–O–C bridge.[21] The representative characteristic peaks of pristine **SP-COOH** are $-CH_3$: 2967, 2870, 1446, 1380; $-CH_2-$: 2926, 1332; C=O: 1710; −C=C−: 1652, 949, 919; Ar–C: 1608, 1578, 1485; O=C–C: 1332; −C−O−C−: 1090. In the FTIR spectrum of the complex **SP-COOH@γCD**, the corresponding characteristic bands belonging to **γCD** were observed at 1027, 1086 and 1159 cm^{-1} respectively. The characteristic peaks of **SP-COOH** are shifted or could not be observed because the formation of inclusion complex suppresses the molecular vibration of **SP-COOH** molecule in **γCD** cavity. The most striking feature for **SP-COOH@γCD** is the concomitant appearance of a new stretching frequency at ν(C=O)=1680 cm^{-1} assigned to hydrogen-bonded carbonyl groups, along with a decrease in the intensity of the band at ν(C=O)=1710 cm^{-1} as a result of stretching vibrations of non-hydrogen-bonded carbonyl groups.[22] The shifted peak at about 3400 cm^{-1} in the FTIR spectrum of **SP-COOH@γCD** can be assigned to the hydrogen-bonded O-H stretching mode, also suggests that strong hydrogen bonds exist in this complex system.[23] Therefore the hydrogen bonds can form not only between hydroxyls of **γCD**, but also between hydroxyls of **γCD** and carboxyls of **SP-COOH**.

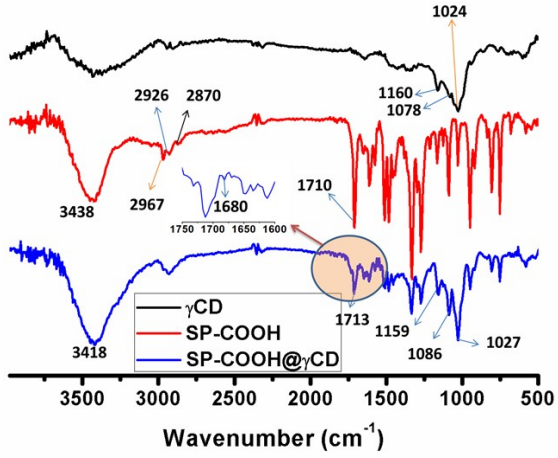

Fig. 4 FTIR spectra of the precursor **γCD**, **SP-COOH**, and the complex **SP-COOH@γCD**.

To explore the hydrogen bonds in strengthening the interactions between the host and guest, NaOH was added into **SP-COOH@γCD** to neutralize the –COOH into –COONa. It was observed that the morphology of complex **SP-COOH@γCD** underwent a dramatic change from well-organized 1D rod-like microcrystal to irregular scattered spot morphology (Fig. 5), suggesting the disassembly of **SP-COOH@γCD**. These changes suggest a crucial role of hydrogen bonds in gathering the isolated complex units. Obviously, the intermolecular hydrogen bond interaction acted as a major driving force for the formation of self-assembled composites.

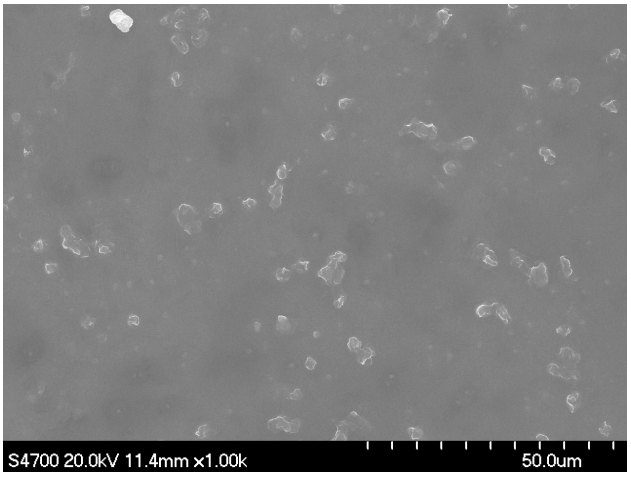

Fig. 5 SEM image of **SP-COOH@γCD** after the addition of NaOH.

3.3 Light-driven fluorescence change, polarized and two-photon-excited fluorescence in the solid state of SP-COOH@γCD

To further investigate the light-controlled absorption and fluorescence properties and to develop potential solid-state device application, the **SP-COOH@γCD** microstructure was further constructed into a thin film by a spin-casting method. The same method was used to produce pure **SP-COOH**, **γCD** and **SP-COOH/γCD** mixture (1:1) film as comparisons for further detection (Fig. S11). The in-situ UV-vis spectra were used to monitor the change in the absorption properties before and after UV (365 nm) irradiation, which show that the characteristic band belonging to **SP-COOH** at 554 nm has a sharp increasing in the beginning and then tends to slow down at ca. 100 seconds (irradiation time). Such behavior can be clearly revealed by the color change from yellow to purple as shown in Fig. 6A. Moreover, the fluorescence has also changed obviously: the initial emission is located at ca. 620 nm, suggest that there already exits slight ring-opened form of **SP-COOH** that is caused by the UV light irradiation during the emission measurement, while after UV radiation for 5 minutes, the emission reaches a maximum and shifts to 663 nm. The occurrence of the strong red fluorescence is assigned to the isomerization from closed-form **SP** to the open-form **PM** state in **γCD** cavity, and the red-shift emission upon the increasing irradiation time can be related to the molecular rearrangement of **PM** and the change in the stack mode.[24, 25] Thus, the fluorescence wavelength and intensity of **SP-COOH@γCD** could be tuned by controlling UV irradiation time.

Journal Name

ARTICLE

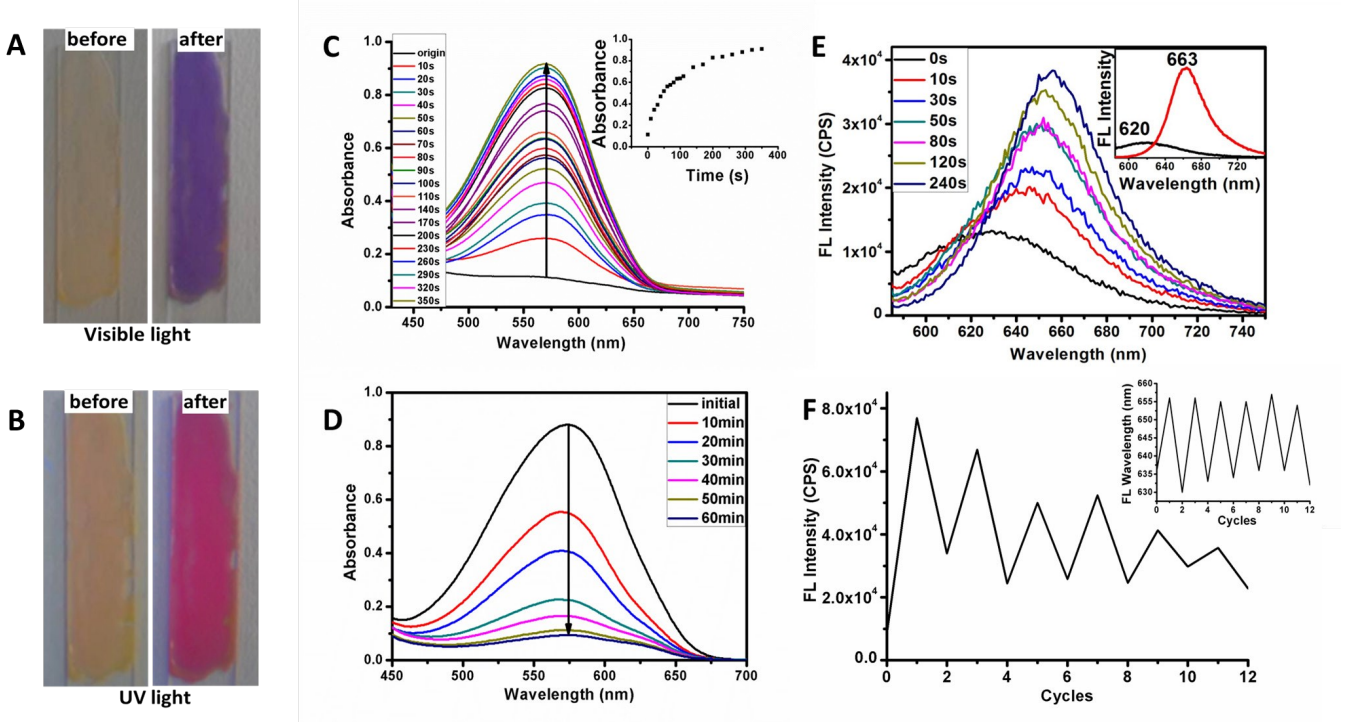

Fig. 6 (A) and (B) describe reversible colour changes of **SP-COOH@γCD** film before (left) and after (right) UV-irradiation: (A) under visible light, (B) under UV light. (C) Time-dependent UV-vis absorption spectra of **SP-COOH@γCD** film. Inset: The tendency of absorbance changing with time. (D) The absorbance decay of **SP-COOH@γCD** film under visible light. (E) Time-dependent emission spectra of **SP-COOH@γCD** film. Excitation = 565 nm, λ_{max} (red shift). Inset: Contrast of minimum intensity and maximum intensity. (F) Fluorescent intensity switch cycles upon alternating irradiation with UV and visible light. Each cycle is under UV (365 nm) irradiation for 3 minutes and then visible light irradiation for 3 hours. Inset: emissive wavelength maximum cycles between 620 and 663 nm.

To verify the repeatable use of the film, absorption and fluorescence cycles are further made. For the absorption spectra, the band at 554 nm can be recovered to its initial state after 60 minutes under visible light. For the fluorescence, the emissive wavelength between 620 and 663 nm can also be recycled easily for several times by alternating irradiation with UV and visible light (Fig. 6F). It should also be noted that neither of the pristine **SP-COOH**, **γCD** nor **SP-COOH/γCD** mixture (1:1) film presents similar color or fluorescence change under the same condition (Fig. S11). Therefore, the formation of complex between **γCD** and **SP-COOH** can achieve an effective light-driven fluorescence change in a reversible manner.

Moreover, compared with the solution and other as-reported systems[26, 27], the produced **SP-COOH@γCD** film after UV irradiation presents a higher PLQY value (Φ_F=17.90%), which solves the problem on solid-state quenching for typical fluorescent dye molecules and also guarantees it as potential UV detector and optical information storage. For the open-ring state of **SP-COOH@γCD**, the well-organized film also presents a highly anisotropic emission, as confirmed by polarized fluorescence spectra (Fig 7A). The fluorescence anisotropy value is ca. 0.18 at 660 nm between I_{VV} and I_{VH} direction, indicating a high degree of **SP-COOH** molecular arrangement within **γCD**.

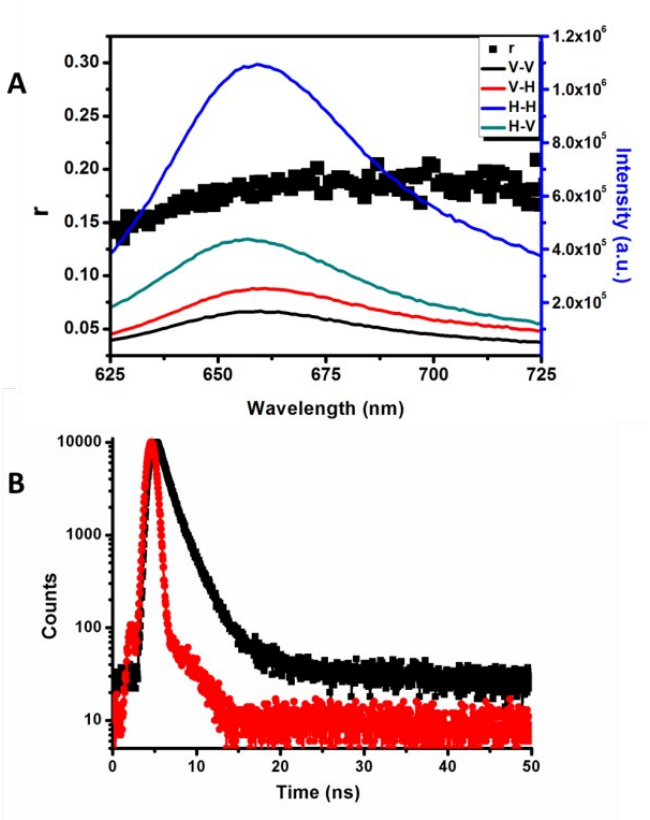

Fig. 7 (A) Polarized fluorescence profiles in the VV, VH, HH, HV modes and anisotropic values for the as prepared **SP-COOH@γCD** film. (B) Fluorescence decay curves of **SP-COOH@γCD** film.

The fluorescence lifetime was also measured and the corresponding fluorescence decay curve is shown in Fig. 7B. Double exponential form was used to fit the decay curve to result in a high accuracy (χ^2=1.006), and the fluorescence lifetime reaches 1.48 ns. This value is comparable to the pristine **SP-COOH** solution system. We noted that the open-ring state of **SP-COOH@γCD** microcrystal can be a two-photon absorption and emissive chromophore, and thus two-photon excited fluorescence measurements were further made. Upon excitation by an 800 nm laser light, **SP-COOH@γCD** exhibits strong two-photon fluorescence without obvious red- or blue-shift emission compared with those excited at UV light (Fig. 8), illustrating that the same emission process from one-photon and two-photon excited states to the ground state are involved. The two-photon emission can be easily imaged under a two-photon fluorescence microscopy (inset in Fig. 8). Therefore, it can be concluded that the light-driven solid-state **SP-COOH@γCD** film system can also serve as polarized fluorescence and two-photon fluorescent materials.

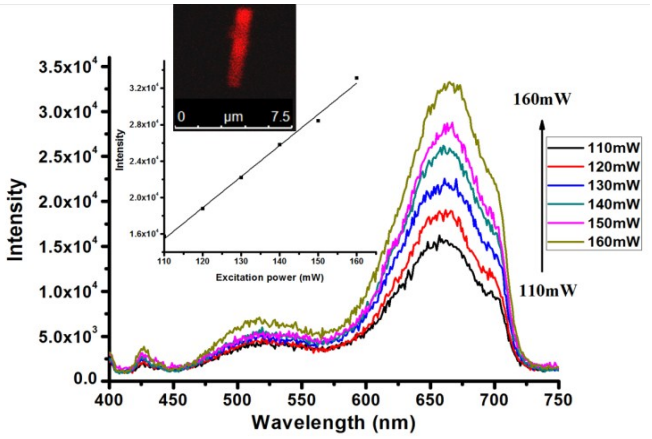

Fig. 8 Two-photon fluorescence spectra of the **SP-COOH@γCD** powder excited by a laser (800 nm). Inset: single microcrystal observed using two-photon fluorescence microscopy.

4. Conclusion

In conclusion, a 1D self-assembled microcrystal system has been developed by the inclusion of **SP-COOH** into **γCD** cavity. The hydrophobic and hydrogen bond interactions between hydroxy in **γCD** and carboxyl in **SP-COOH** play an important role in the formation of the 1D microstructure. The **SP-COOH@γCD** system presents both photochromism and light-driven fluorescence change (both the intensity and wavelength) upon UV light irradiation, due to the transformation from close- to open-ring state as well as the change of stacking mode of **SP-COOH** within **γCD**. For the open-ring state, the **SP-COOH@γCD** microcrystal also presents polarized emission and two-photon-excited fluorescence; its high fluorescent quantum yield also solves the solid-state aggregation quenching for the typical **SP** molecule. The solid state color and fluorescence of the host-guest assemblies was effectively switched by alternate irradiation with UV and

visible light. Therefore, this work supplies an effective way to achieve **SP**-based microcrystal materials with a reversible light-driven fluorescence change.

Acknowledgements

This work was financially supported by the National Natural Science Foundation of China (21174012, 51221002, 21301016, and 21473013), the Beijing Natural Science Foundation (2142026), and the Innovation and Promotion Project of Beijing University of Chemical Technology.

Notes and reference

1. R. Friend, R. Gymer, A. Holmes, J. Burroughes, R. Marks, C. Taliani, D. Bradley, D. Dos Santos, J. Bredas and M. Lögdlund, *Nature*, 1999, **397**, 121-128.
2. C. Zhang, C. Zou, Y. Yan, R. Hao, F. Sun, Z. Han, Y. S. Zhao and J. Yao, *J. Am. Chem. Soc.*, 2011, **133**, 7276-7279.
3. a) M. Chen and M. Yin, Prog. Polym. Sci., 2014, 39 , 365-395; b) L. Hao, J. Ning, B. Luo, B. Wang, Y. Zhang, Z. Tang, J. Yang, A. Thomas and L. Zhi, *J. Am. Chem. Soc.,* 2014, **137**, 219-225.
4. a) D. Yan, J. Lu, M. Wei, S. Li, D. G. Evans and X. Duan, *Phys. Chem. Chem. Phys.*, 2012, **14**, 8591-8598; b) D. Yan, W. Jones, G. Fan, M. Wei and D. G. Evans, *J. Mater. Chem. C*, 2013, **1**, 4138–4145; c) R. Gao, M. Zhao, Y. Guan, X. Fang, X. Li, and D. Yan, *J. Mater. Chem. C*, 2014, **2**, 9579-9586.
5. a) J. W. Chung, S. J. Yoon, S. J. Lim, B. K. An and S. Y. Park, *Angew. Chem.*, 2009, **121**, 7164-7168; b) M. Frenette, G. Cosa and T. Friščić, *CrystEngComm,* 2013, **15**, 5100-5106.
6. a) O. Bolton, K. Lee, H. Kim, K. Y. Lin and J. Kim, *Nat. Chem.*, 2011, **3**, 205-210; b) R. Gao, D. Cao, Y. Guan and D. Yan. *ACS Applied. Mater. Inter.,* 2015, **7**, 9904-9910; c) H. Nie, G. Sun, M. Zhang, M. Baumgarten and K. Müllen, *J. Mater. Chem.,* 2012, **22**, 2129-2132.
7. X. Peng, J. Deng and H. Xu, *RSC Adv.*, 2013, **3**, 24146-24153.
8. G. K. Such, R. A. Evans and T. P. Davis, *Macromolecules*, 2006, **39**, 9562-9570.
9. N. Shao, J. Y. Jin, S. M. Cheung, R. H. Yang, W. H. Chan and T. Mo, *Angew. Chem.*, 2006, **118**, 5066-5070.
10. P. Belser, L. De Cola, F. Hartl, V. Adamo, B. Bozic, Y. Chriqui, V. M. Iyer, R. T. Jukes, J. KüHNI and M. Querol, *Adv. Funct. Mater.*, 2006, **16**, 195-208.
11. S. Wan, Y. Zheng, J. Shen, W. Yang and M. Yin, *ACS Appl. Mater. Inter.*, 2014, **6**, 19515-19519.
12. S. Iyengar and M. C. Biewer, *Cryst. Growth. Des.*, 2005, **5**, 2043-2045.
13. a) L. Wang, J. Chen and J. Chen, *Mater. Chem. Phys.*, 2012, **136**, 151-159; b) M. Zhu, T. Chen, G. Zhang, C. Li, W. Gong, Z. Chen and M. P. Aldred, *Chem. Commun.*, 2014, **50**, 2664-2666; c) M. Zhu, G. Zhang, Z. Hu, M. P. Aldred, C. Li, W. Gong, T. Chen, Z. Huang and S. Liu, *Macromolecules.*, 2014, **47**, 1543-1552.
14. a) Q. Song, Z. Luo, Y. Du and Y. Huang, *Chin. J. Polym. Sci.*, 2014, **32**, 1003-1009; b) S. P. Newman, T. Di Cristina, P. V. Coveney and W. Jones, *Langmuir,* 2002, **18**, 2933-2939.
15. a) A. Douhal, *Chem. Rev.*, 2004, **104**, 1955-1976; b) G. R. Williams, A. Clout and J. C. Burley, *Phys. Chem. Chem. Phys.,* 2013, **15**, 8616-8628.
16. T. Tamaki, M. Sakuragi, K. Ichimura, K. Aoki and I. Arima, *Polym. Bull.*, 1990, **24**, 559-564.
17. S. Zhang, M. Fan, Y. Liu, Y. Ma, G. Zhang and J. Yao, *Langmuir*, 2007, **23**, 9443-9446.
18. Y. Sueishi and T. Miyakawa, *J. Phys. Org. Chem.*, 1999, **12**, 541-546.
19. G. g. Crini, *Chem. Rev.*, 2014, **114**, 10940-10975.
20. Y. Hu, Y. Liu and X. Xiao, *Biomacromolecules*, 2009, **10**, 517-521.
21. M. Chen, S. R. Nielsen, T. Uyar, S. Zhang, A. Zafar, M. Dong and F. Besenbacher, *J. Mater. Chem. C*, 2013, **1**, 850-855.
22. T. E. Kaiser, H. Wang, V. Stepanenko and F. Würthner, *Angew. Chem. Int. Ed.*, 2007, **46**, 5541-5544.
23. J. Zhang, M. Zhou, S. Wang, J. Carr, W. Li and L. Wu, *Langmuir*, 2011, **27**, 4134-4141.
24. A. Datar, K. Balakrishnan, X. Yang, X. Zuo, J. Huang, R. Oitker, M. Yen, J. Zhao, D. M. Tiede and L. Zang, *J. Phys. Chem. B,* 2006, **110**, 12327-12332.
25. P. Yan, A. Chowdhury, M. W. Holman and D. M. Adams, *J. Phys. Chem. B,* 2005, **109**, 724-730.
26. Z. Li, S. Wan, W. Shi, M. Wei, M. Yin, W. Yang, D. G. Evans and X. Duan, *J. Phys. Chem. C*, 2015, **119**, 7428-7435.
27. M. Li, W. Yao, J. Chen, H. Lu, Y. Zhao and C. Chen, *J. Mater. Chem. C,* 2014, **2**, 8373-8380.

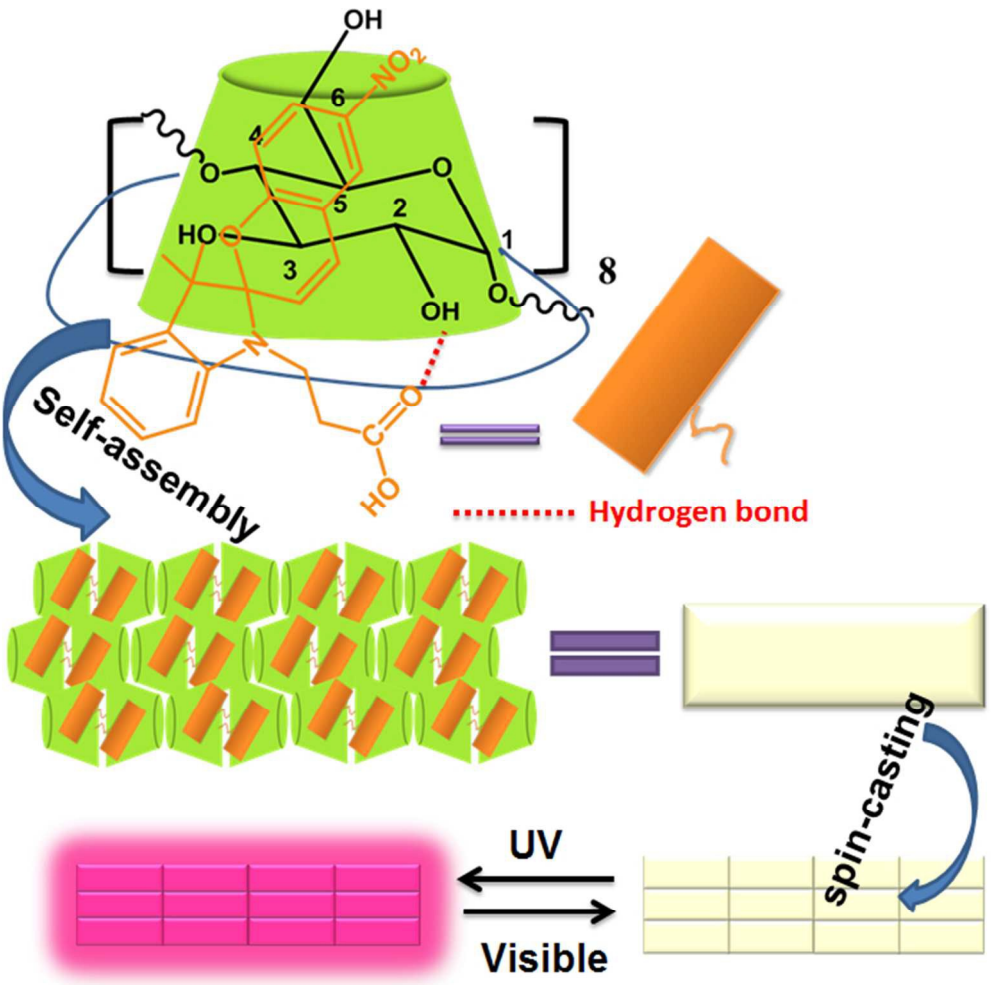

One-dimentioanal (1D) solid-state microcrystals combining the host cyclodextrin (CD) and UV-responsive guest molecule spiropyran (SP) present a light-driven fluorescence change based on the isomerization of the SP molecule in the CD matrix.
186x187mm (95 x 95 DPI)